TURN-BY-TURN MEASUREMENTS FOR SYSTEMATIC INVESTIGATIONS OF THE MICRO-BUNCHING INSTABILITY[*]

J. L. Steinmann[†], M. Brosi, E. Bründermann, M. Caselle, S. Funkner, B. Kehrer,
M. J. Nasse, G. Niehues, L. Rota, P. Schönfeldt, M. Schuh, M. Siegel, M. Weber and A.-S. Müller
Karlsruhe Institute of Technology, Karlsruhe, Germany

Abstract

While recent diffraction-limited storage rings provide bunches with transverse dimensions smaller than the wavelength of the observed synchrotron radiation, the bunch compression in the longitudinal plane is still challenging. The benefit would be single cycle pulses of coherent radiation with many orders of magnitude higher intensity. However, the self-interaction of a short electron bunch with its emitted coherent radiation can lead to micro-bunching instabilities. This effect limits the bunch compression in storage rings currently to the picosecond range. In that range, the bunches emit coherent THz radiation corresponding to their bunch length. In this paper, new measurement setups developed at the Karlsruhe Institute of Technology are described for systematic turn-by-turn investigations of the micro-bunching instability. They lead to a better understanding thereof and enable appropriate observation methods in future efforts of controlling and mastering the instability. Furthermore, the described setups might also be used as high repetition rate bunch compression monitors for bunches of picosecond length and below.

MICRO-BUNCHING INSTABILITY

The micro-bunching instability (MBI) is a longitudinal instability that arises due to the self-interaction of a bunch with its emitted electro-magnetic field[1]. This interaction can be modelled by a synchrotron-radiation impedance whose real part corresponds to the emitted radiation. The impedance has a low frequency cutoff due to the shielding of the vacuum chamber [2] and a high frequency cutoff due to the particle energy. The shielded wavelengths can be approximated with the shielding cutoff $\lambda = 2h\sqrt{h/R}$ with h being the beam pipe height and R the particles radius of curvature, while the high frequency cutoff can be approximated by the critical frequency of the synchrotron radiation $f_c = 3\gamma^3 c/(4\pi R)$. Therefore, the impedance has significant strength if $\gamma^3\sqrt{h^3 R^{-3}} \gtrsim 2$. While this applies to almost all light sources, only a few heavy particle machines reach high enough energies. However, also future colliders will be confronted with high amount of synchrotron radiation.

In order to generate a significant wake potential, the bunch spectrum and the impedance need to overlap. As a rule of thumb, storage rings with a few meters bending radius and some tens of centimeters beam-pipe height typically have a cutoff around hundred gigahertz, leading to a critical bunch length around ten picoseconds. At first, the additional wake potential leads to potential well distortion and a change of bunch shape. Then, above a critical bunch charge, a self-amplified system is formed since the distorted bunch shape increases the wake potential further. This leads to the formation of sub-structures on the bunch profile and a blow-up of the bunch in phase space. The blow-up is much faster and stronger than the damping time and no equilibrium is reached. The bunch is blown up, until the wake potential becomes negligible. Then, the radiation damping shortens the bunch, until the threshold is hit again. Consequently, a sawtooth behaviour is observed.

Due to the characteristic bunch size of a few picoseconds and even smaller substructures, signatures of the instability can be seen in the terahertz frequency range where outbursts of coherent radiation are observed. Obviously, the behaviour is beam current dependent, too.

The relevant time scales when observing the MBI reach from a few turns during the start of a burst, over some milliseconds between consecutive bursts, to minutes and hours when analyzing current dependent changes. Consequently, the diagnostics need to be single shot, turn-by-turn and be able to record for long time scales. In this paper, we will present recent diagnostic systems developed and evaluated at the Karlsruhe Institute of Technology (KIT).

KARLSRUHE RESEARCH ACCELERATOR

The Karlsruhe Research Accelerator (KARA) is the 2.5 GeV storage ring of the KIT. It can be varied for a broad range of parameters (see Table 1). A special short-bunch mode is established at 1.3 GeV.

Table 1: KARA Parameters

L	110.4	m
f_{RF}	499.7	MHz
h	32	mm
Energy	0.5 to 2.5	GeV
V_{RF}	150 to 1500	kV
α_c	1.6×10^{-4} to 1×10^{-2}	
$\sigma_{z,0}$	1.9 to 45	ps

[1] For a good summary of the topic see Ref. [1].

TUP2WD03

D - Key Technologies

THz DIAGNOSTICS USING KAPTURE

KAPTURE (KArlsruhe Pulse Taking and Ultrafast Read-out Electronics)[3–5] is an in-house built DAQ system for ultra-fast detector pulses with a bunch-to-bunch repetition rate. It uses the memory efficient approach to only sample and store the detector pulse, neglecting the noise in-between. In contrast to state-of-the-art oscilloscopes, the 4 GBytes/s of raw data can be streamed out continuously to the readout computer via PCI-Express.

KAPTURE consists of four 12-bit ADCs whose sampling trigger points can be adjusted in 3 ps steps each. Several operation modes can be configured.

The standard mode allows the reconstruction of the detector pulse amplitude and the arrival time. For this, the detector is connected to a 1-to-4 splitter, distributing the detector signal to the four sampling channels. By setting the individual delays of the channels, the pulse can be sampled with up to 330 GSa/s local sampling rate.

Another operation mode is the use of four individual detectors instead of the output of the power splitter. In this way the pulse amplitudes of the detector responses of all detectors are intrinsically sampled synchronously. This allows the operation as single-shot spectrometer, when detectors sensitive in different frequency ranges are used. However, only a single sampling point per detector and pulse is taken.

Snapshot Measurements

By using KAPTURE and a fast THz detector, the outbursts of radiation due to the MBI can be studied turn-by-turn and even bunch-by-bunch. Figure 1 shows raw data of a broadband THz detector recorded with KAPTURE. The intensity fluctuations are clearly visible for each bunch. Depending on their bunch current, the bunches display different bursting behaviors, i.e., the temporal evolution of a burst and the repetition rate.
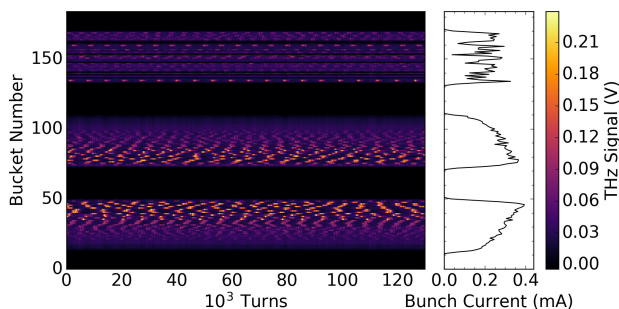

Figure 1: The fluctuating THz signal (color-coded) of each of the 184 RF buckets is shown for 130 thousand consecutive turns. The bursting behavior differs for bunches with different currents. The right hand side shows the filling pattern, consisting of three trains [6].

Usually, the dynamics of the MBI are shown in a spectrogram, where the fluctuations at a given bunch current are measured. The conventional procedure, involving a single bunch, takes hours of measurement time, where the bunch charge is changed between measurements. With KAPTURE providing a bunch-by-bunch sampling, the measurement time can be shortened drastically [6] by using the information from multiple bunches at once. To cover the current range of interest, a tailored filling pattern (see right panel of Fig. 1) is created with a bunch-by-bunch feedback system [7]. By sorting the bunch signals by their charge, the current dependent effects can be studied by a single acquisition.

This method was used to quickly map the instability thresholds as well as the bounds of the short bunch-length bursting (SBB) (a weak instability, further information in [8, 9]) for different settings of the RF voltage and the momentum compaction factor α_c [9]. The resulting thresholds are displayed in Fig. 2 together with the prediction from a simulation by Bane, Cai, and Stupakov [8] using the dimensionless parameters CSR strength $S_{CSR} = I_n R^{1/3} \sigma_{z,0}^{-4/3}$ and shielding factor $\Pi = \sigma_{z,0} R^{1/2} h^{-3/2}$ (following the definition in [8, 9]).
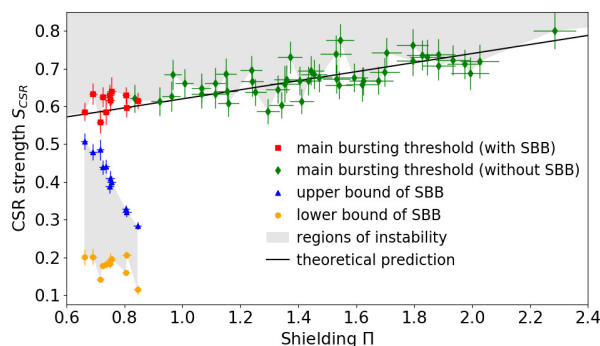

Figure 2: The MBI threshold displayed in CSR strength as a function of the shielding parameter for measurements at different machine parameters. The prediction by [8] is shown as black line. The error bars display the standard deviation error of the measurements [9].

4-Channel Spectrometer

Another operation mode of KAPTURE is the use of different detectors in parallel. With its four sampling channels, up to four detectors can be read out synchronously by KAPTURE. The setup presented here consists of four waveguide coupled Schottky detectors, each sensitive in a different frequency range. The synchrotron radiation is coupled out at the diagnostic port of the IR2 beamline and split with wire grids into four equal parts, each focused to an individual detector. Such a setup is depicted in Fig. 3.

An example measurement of a radiation outburst, detected with four diodes simultaneously, is shown in Fig. 4. A different phase of the periodic signals is observed, indicating changing spectral components.

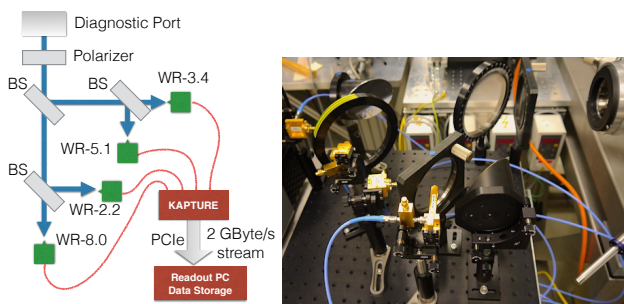For more information see Refs. [10, 11].

Figure 3: The synchrotron radiation emitted at the diagnostic port is first polarized and then divided into four beams by three wire-grid beam splitters (BS). The split beams are focused onto four detectors, each one sensitive in a different frequency band. The single-shot measurements are sampled and read out by the KAPTURE system.
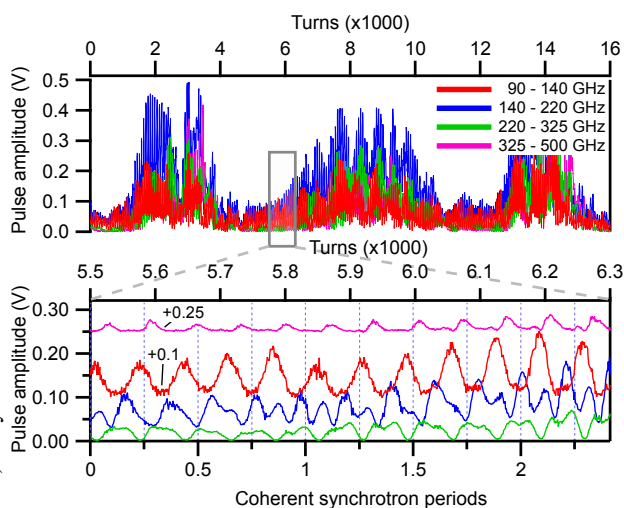

Figure 4: KAPTURE allows the continuous readout of four detectors in parallel. Each detector is sensitive in a different frequency range, leading to a four-channel single-shot spectrometer. A phase shift between the different frequencies can be observed in the zoom-in.

ELECTRO-OPTICAL BUNCH PROFILE MEASUREMENTS

To measure the longitudinal bunch profile we use our permanently installed electro-optical (EO) near-field setup. The fundamental detection scheme was first demonstrated in [12]. In 2013, we installed the first, and up to now only, EO near-field setup in a storage ring [13]. The layout (EOS v1) was identical to the design originally developed for the SwissFEL injector test facility [14] at PSI.

The electro-optical spectral decoding (EOSD) setup combined with the ultra-fast line camera KALYPSO (described below) as spectrometer allows turn-by-turn single-shot measurements. The working principle of this method is depicted in Fig. 5: A vertically polarized laser pulse (1) is first sent through a polarization-maintaining dispersive fiber (2). Thereby, the fs laser pulses are stretched to picosec-
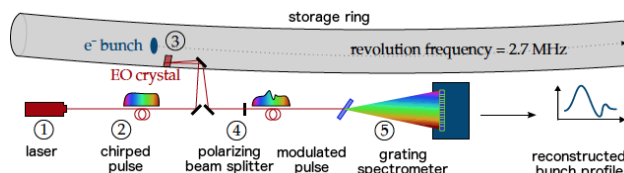

Figure 5: Working principle of the EO setup. See text for details. [15]

onds resulting in a frequency chirp. Inside an EO crystal (3), brought in close vicinity to the electron beam, the polarization of the laser pulse is changed depending on the electrical field present. Due to the chirp the temporal profile of the electron bunch is encoded in the frequency profile of the laser pulse. Using a polarizing beam splitter (4), the polarization modulation is turned into an intensity modulation that can be probed using a spectrometer (5). To be precise, the refractive index of the crystal is $n_0 > 1$, so what is actually measured is not the Coulomb field of the electrons, but a wakefield created at the crystal surface facing the arriving electrons. Additional electric fields can influence the measurement. The most prominent one in bunch-profile measurements is the part of the Coulomb field penetrating the crystal from the bottom [16]. At later times reflections can occur from various surfaces [17]. When the bunch spacing is too small, these fields can influence the measurement of the next bunch.

In 2016, we optimized the in-vacuum geometry (EOS v2) to account for the needs of a circular accelerator. To achieve a higher signal at low bunch charges, we increased the crystal thickness and reduced the distance between the electron beam and the laser path. This comes at the cost of increased influence of the electric fields coming from the bottom side of the crystal. The new layout was also designed [18] to minimize the effect of remaining wakefields at the position of a consecutive bunch to allow a closer bunch spacing (see Fig. 6).
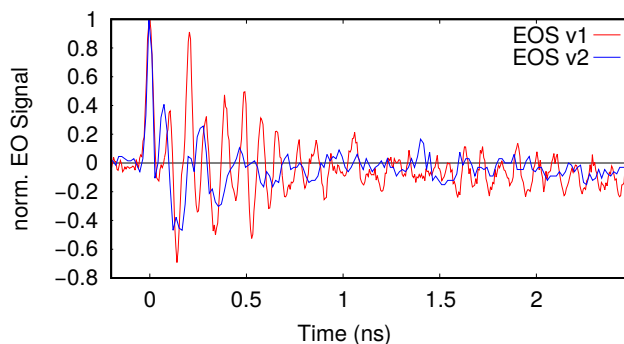

Figure 6: EO measurements performed with the EOS v1 and improved EOS v2 in-vacuum geometry. This comparison clearly shows the reduced trailing wakefields especially at 2 ns, the location of a subsequent bunch during multi-bunch operation. [18]
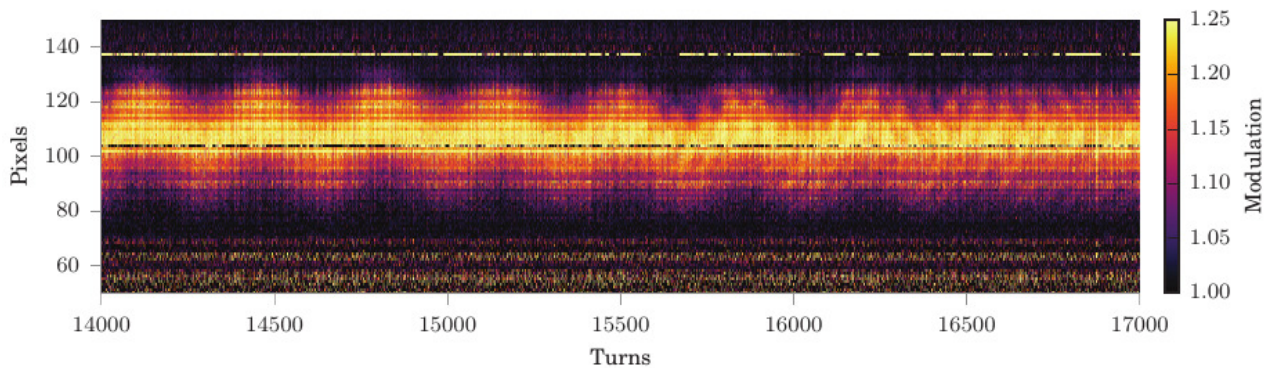
Figure 7: Raw EO measurement data recorded using KALYPSO over multiple turns. The acquisition rate was set to 2.7 Mfps, so that each vertical line corresponds to a single-shot and turn-by-turn measurement of the longitudinal bunch profile. The synchrotron oscillation of the electron bunch is clearly visible. Starting from turn 15500, the formation of substructures due to the MBI can be observed. The full dataset consists of 5×10^5 turns, one turn corresponding to 368 ns. [19]

Using the MHz line-array KALYPSO (KArlsruhe Linear arraY detector for MHz rePetition rate SpectrOscopy) [19] that was developed in collaboration between DESY, PSI, the University of Łódź, and KIT for exactly that purpose, it is now possible to track the longitudinal profile of an individual electron bunch on a turn-by-turn basis for theoretically infinite times without gaps. KALYPSO includes of a photon sensitive line array. Each of the 256 pixels is individually connected to the front-end electronics, allowing a readout rate of 2.7 Mfps. The line array can be based either on Si or InGaAs depending on the desired range of wavelengths. When using silicon, back illumination provides higher quantum efficiency.

The continuous streaming capability with turn-by-turn resolution of this setup is illustrated in Fig. 7. It shows synchrotron oscillation, as well as the formation of substructures due to the MBI in the second half of the panel.

TIME-RESOLVED ENERGY SPREAD STUDIES

As the energy spread cannot be measured directly, it is accessed via the horizontal bunch size in a dispersive region. For the equilibrium state, they are related according to Eq. 1.

$$\sigma_x = \sqrt{\beta_x \cdot \epsilon_x + (D_x \cdot \sigma_\delta)^2} \qquad (1)$$

Therefore, the horizontal beta function and dispersion at the imaging source point as well as the emittance are required. They can be determined using the Accelerator Toolbox for MATLAB [20] and LOCO for fitting the quadrupole strengths [21]. For the equilibrium case below the bursting threshold, where no deformation of the energy profile of the bunch is expected, this leads to reasonable good agreement between the measured horizontal bunch size and the calculated one according to Eq. 1.

To allow for time-resolved studies of the horizontal bunch size we are using a setup based on a fast-gated intensified camera (FGC) [22] located at the visible light diagnostics port [23]. The combination of the gating function of the

camera and a fast, rotating mirror allows single-turn images of one bunch, see Fig. 8 for the principle scheme of this process.
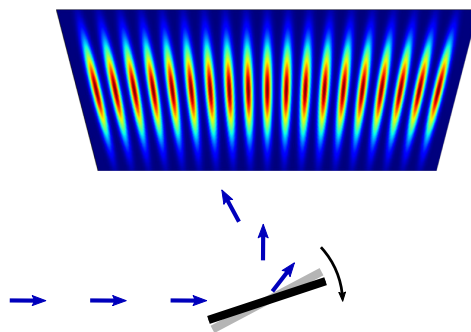

Figure 8: Functional principle of the rotating mirror. It sweeps the incoming light over the sensor of the camera. Due to the gating of the camera, a single bunch can be tracked in a multi-bunch environment.

On the current camera sensor, up to 60 individual spots can be analyzed. A minimum separation of 6 turns is achieved between two spots, due to the revolution frequency of 2.7 MHz and the rotation speed of the mirror.

The final image on the FGC sensor is the convolution of the charge distribution and the filament beam spread function (FBSF). The FBSF is the extension of the point spread function for a moving source. It is determined from simulations of the imaging process using the software OpTalix [24]. To overcome the problems coupled to a deconvolution (e.g. a correct estimation of the signal-to-noise ratio) we fit a convolution of a Gaussian curve with the FBSF to the spot profiles to get a measure for the horizontal bunch size.

For a single spot and its profile, such a fit is illustrated in Fig. 9.

The setup is embedded into the hardware synchronization scheme [25] and thus enables simultaneous studies of the energy spread and the CSR emission. One example for such a synchronized measurement is illustrated in Fig. 10.
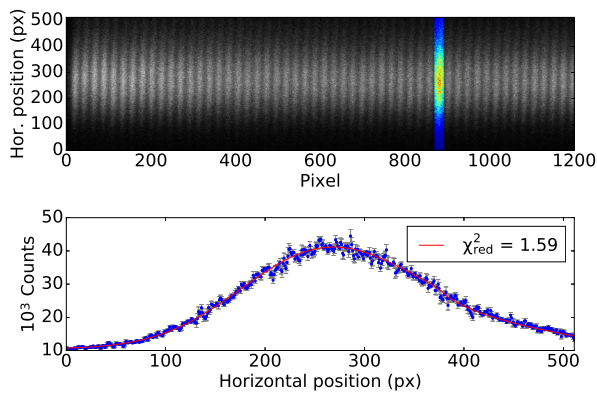
Figure 9: Top: Raw image of the FGC showing 53 single-turn images (spots) of the same bunch, each separated by 500 turns. For one spot, highlighted in color, the corresponding horizontal profile as well as the fit are shown on the bottom.
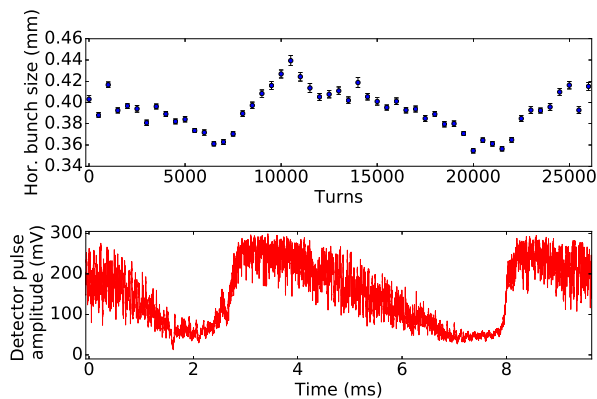

Figure 10: Horizontal bunch size as a measure for the energy spread (top) and the simultaneously recorded CSR intensity using a broadband Schottky diode (bottom). [26]

It shows that the energy spread as well as the CSR intensity perform a modulation with the same period length. At the onset of CSR burst, the energy spread reaches a minimum and is blown up in the following until a certain limit is reached, where damping effects start to dominate leading to a shrinking of the energy spread. This shrinking holds until a certain lower level is reached, where the energy spread hits a lower threshold coupled to the onset of the next burst (see [26]).

SUMMARY AND OUTLOOK

The micro-bunching instability (MBI) limits the reduction of the bunch length in a storage ring. To analyze this instability, we have set up and developed several single-shot high repetition-rate diagnostics stations. We have presented an overview of our various diagnostic methods to analyze the emitted CSR, the energy spread, and the longitudinal bunch profile. These diagnostic stations allow the synchronous analysis of the longitudinal phase space, and enable new insights into the dynamics of the MBI. Our findings also in-

fluence the development of our open-source Vlasov-Fokker-Planck solver Inovesa [27], which reproduces most features of the MBI remarkably well.

The development of the in-house readout electronics is still ongoing, both for KAPTURE and KALYPSO. A version 2 of KAPTURE is already being commissioned [28]. It not only doubles the number of sampling channels to eight, but also the sampling rate of each ADC to 1 GSa/s. This will improve both discussed readout modes, because more detectors can be readout synchronously or a better reconstruction of the detector pulse can be achieved. Furthermore, the sampling of the baseline in-between the pulses is enabled to improve accuracy by removing baseline fluctuations and lower frequency noise.

The four-channel spectrometer setup with individual detectors can hardly be expanded to more detectors as it is limited by space, intensity, and frequency bandwidth. To overcome this issue, at KIT an integrated planar array of super-conducting Y-Ba-Cu-O detectors, to be used with KAPTURE, is developed [29, 30].

Upcoming versions of KALYPSO include a 10 Mfps read-out with less than 300 electrons equivalent-noise-charge and new line arrays with 512, 1024 or 2048 pixels as well as with a pitch of 25 μm or 45 μm. The anti-reflection coatings can be optimized for near-infrared (1050 nm), visible (400 nm to 850 nm) and near-ultraviolet (350 nm).

This makes it possible to use KALYPSO for a very wide range of different applications, not only in the field of accelerator physics. In the near future, we will use it for horizontal bunch size measurements in the visible frequency range as well. This overcomes the intrinsic limits of the FGC setup (no turn-by-turn capability, limited number of spots per image) and will allow continuous turn-by-turn studies of the energy spread. First tests were already successful.

KAPTURE and KALYPSO share the same readout architecture. A newly developed high-throughput architecture based on PCI-Express Gen3 and DirectGMA technology will be used to stream data directly to a GPU. This approach has about five times less data latency than other DMA architectures and permits realtime calculations on the GPU and enables their use for beam feedback [31]. Pre-processing before data storage is also a viable option for data reduction of the potentially large amount of data from various sensors and detector systems.

REFERENCES

[1] W. C. C. Biscari, in *ICFA Beam Dynamic Newsletter*, vol. 35, 2004,
URL: http://icfa-usa.jlab.org/archive/newsletter/icfa_bd_nl_35.pdf

[2] T. Agoh, "Steady fields of coherent synchrotron radiation in a rectangular pipe," *Phys. Rev. ST Accel. Beams*, vol. 12, p. 094 402, 9 Sep. 2009,
DOI: 10.1103/PhysRevSTAB.12.094402.

[3] M. Caselle *et al.*, "Commissioning of an Ultra-fast Data Acquisition System for Coherent Synchrotron Radiation De-

tection," in *Proceedings of 2014 International Particle Accelerator Conference*, 2014.

[4] M. Caselle *et al.*, "An ultra-fast data acquisition system for coherent synchrotron radiation with terahertz detectors," *Journal of Instrumentation*, vol. 9, no. 01, p. C01024, 2014, DOI: 10.1088/1748-0221/9/01/C01024.

[5] M. Caselle *et al.*, "An ultra-fast digitizer with picosecond sampling time for Coherent Synchrotron Radiation," in *19th IEEE-NPSS Real Time Conference*, May 2014, pp. 1–3, DOI: 10.1109/RTC.2014.7097535.

[6] M. Brosi *et al.*, "Fast mapping of terahertz bursting thresholds and characteristics at synchrotron light sources," *Phys. Rev. Accel. Beams*, vol. 19, p. 110 701, 11 Nov. 2016, DOI: 10.1103/PhysRevAccelBeams.19.110701.

[7] E. Hertle, E. Huttel, A.-S. Müller, N. Smale, D. Teytelman, and M. Höner, "First Results of the new bunch-by-bunch feedback system at ANKA," in *Proceedings of 2014 International Particle Accelerator Conference*, 2014, p. 1739.

[8] K. L. F. Bane, Y. Cai, and G. Stupakov, "Threshold studies of the microwave instability in electron storage rings," *Phys. Rev. ST Accel. Beams*, vol. 13, p. 104 402, 10 Oct. 2010, DOI: 10.1103/PhysRevSTAB.13.104402.

[9] M. Brosi *et al.*, "Systematic Studies of Short Bunch-Length Bursting at ANKA," in *Proceedings, 7th International Particle Accelerator Conference (IPAC 2016)*, Jun. 2016, pp. 1662–1665, DOI: doi:10.18429/JACoW-IPAC2016-TUPOR006.

[10] J. L. Steinmann *et al.*, "Time Resolved Spectral Analysis of Coherent Synchrotron Radiation using a sub-THz 4-Channel Single Shot Spectrometer with 500 MHz Repetition Rate and Continuous Readout," arXiv:1710.09568, 2017, URL: https://arxiv.org/abs/1710.09568

[11] J. Steinmann *et al.*, "4-Channel Single Shot and Turn-by-Turn Spectral Measurements of Bursting CSR," in *Proceedings, 8th International Particle Accelerator Conference (IPAC 2017)*, May 2017, pp. 231–234, DOI: 10.18429/JACoW-IPAC2017-MOPAB056.

[12] I. Wilke, A. M. MacLeod, W. A. Gillespie, G. Berden, G. M. H. Knippels, and A. F. G. van der Meer, "Single-Shot Electron-Beam Bunch Length Measurements," *Phys. Rev. Lett.*, vol. 88, p. 124 801, 12 Mar. 2002, DOI: 10.1103/PhysRevLett.88.124801.

[13] N. Hiller *et al.*, "electro-optical bunch-length measurements at the anka storage ring."

[14] B. Steffen, V. Schlott, and F. Müller, "A compact single shot electro-optical bunch length monitor for the SwissFEL," in *Proceedings of DIPAC09*, (Basel, Switzerland), 2009, URL: https://diagnostics.web.psi.ch/publications/DIPAC09_TUPB42.pdf

[15] L. Rota, "KALYPSO, a novel detector system for high-repetition rate and real-time beam diagnostics," PhD thesis, Karlsruhe Institute of Technology, 2017.

[16] S. Jamison *et al.*, "Electro-optic techniques for temporal profile characterisation of relativistic Coulomb fields and coherent synchrotron radiation," *Nuclear Instruments and Methods in Physics Research Section A: Accelerators, Spectrometers, Detectors and Associated Equipment*, vol. 557, no. 1, pp. 305–308, 2006, DOI: 10.1016/j.nima.2005.10.090.

[17] Q. Wu and X. Zhang, "Free-space electro-optic sampling of terahertz beams," *Applied Physics Letters*, vol. 67, no. 24, pp. 3523–3525, 1995,

DOI: 10.1063/1.114909.

[18] P. Schönfeldt *et al.*, "Towards Near-Field Electro-Optical Bunch Profile Monitoring in a Multi-Bunch Environment," in *Proceedings of the International Particle Accelerator Conference*, May 2017, pp. 227–230, DOI: 10.18429/JACoW-IPAC2017-MOPAB055.

[19] L. Rota *et al.*, "KALYPSO: A Mfps Linear Array Detector for Visible to NIR Radiation," in *Proc. of International Beam Instrumentation Conference (IBIC'16), Barcelona, Spain, Sept. 13-18, 2016*, Sep. 2017, pp. 741–744, DOI: 10.18429/JACoW-IBIC2016-WEPG46.

[20] B. Nash *et al.*, "New functionality for beam dynamics in Accelerator Toolbox (AT)," in *Proceedings of IPAC'15*, 2015, pp. 113–116.

[21] J. Safranek *et al.*, "Theme section - LOCO," *ICFA Beam Dynamics Newsletter*, vol. 44, no. SLAC-REPRINT-2009-545, pp. 43–80, 2009.

[22] P. Schütze, *Transversale Strahldynamik bei der Erzeugung kohärenter Synchrotronstrahlung*. Springer, 2017, ISBN: 978-3-658-20385-6.

[23] B. Kehrer *et al.*, "Visible Light Diagnostics at the ANKA Storage Ring," in *Proceedings of IPAC'15, Richmond, USA*, 2015, pp. 866–868.

[24] Optical Engineering Software, *OpTalix Pro*, http://www.optenso.com, 2013.

[25] B. Kehrer *et al.*, "Simultaneous Detection of Longitudinal and Transverse Bunch Signals at ANKA," in *Proceedings, 7th International Particle Accelerator Conference (IPAC 2016)*, Jun. 2016, pp. 109–111, DOI: doi:10.18429/JACoW-IPAC2016-MOPMB014.

[26] B. Kehrer *et al.*, "Time-Resolved Energy Spread Studies at the ANKA Storage Ring," in *Proceedings, 8th International Particle Accelerator Conference (IPAC 2017)*, May 2017, pp. 53–56, DOI: https://doi.org/10.18429/JACoW-IPAC2017-MOOCB1.

[27] P. Schönfeldt, M. Brosi, M. Schwarz, J. L. Steinmann, and A.-S. Müller, "Parallelized Vlasov-Fokker-Planck solver for desktop personal computers," *Phys. Rev. Accel. Beams*, vol. 20, p. 030 704, 3 Mar. 2017, DOI: 10.1103/PhysRevAccelBeams.20.030704.

[28] M. Caselle *et al.*, "KAPTURE-2. A picosecond sampling system for individual THz pulses with high repetition rate," *Journal of Instrumentation*, vol. 12, no. 01, p. C01040, 2017, URL: http://stacks.iop.org/1748-0221/12/i=01/a=C01040

[29] A. Schmid *et al.*, "Single-Shot Spectral Analysis of Synchrotron Radiation in THz Regime at ANKA," in *Proceedings, 7th International Particle Accelerator Conference (IPAC 2016)*, 2016, DOI: 10.18429/JACoW-IPAC2016-MOPMB016.

[30] A. Schmid *et al.*, "An Integrated Planar Array of Ultra-fast Y-Ba-Cu-O Detectors for Spectroscopic Measurements," *IEEE Transactions on Applied Superconductivity*, vol. 27, no. 4, pp. 1–5, Jun. 2017, DOI: 10.1109/TASC.2016.2625763.

[31] L. Rota *et al.*, "A high-throughput readout architecture based on PCI-Express Gen3 and DirectGMA technology," *Journal of Instrumentation*, vol. 11, no. 02, 2016, URL: http://stacks.iop.org/1748-0221/11/i=02/a=P02007

TUP2WD03